Microelectronics Reliability xxx (2010) xxx–xxx

Contents lists available at ScienceDirect

Microelectronics Reliability

journal homepage: www.elsevier.com/locate/microrel

Structural health monitoring based on continuous ACO method

Ling Yu [a,b,*], Peng Xu [a]

[a] MOE Key Lab of Disaster Forecast and Control in Engineering, Jinan University, Guangzhou 510632, China
[b] Department of Civil Engineering, China Three Gorges University, Yichang 443002, China

ARTICLE INFO

Article history:
Received 12 September 2010
Accepted 13 September 2010
Available online xxxx

ABSTRACT

Structural damage detection remains as a challenging task in the field of structural health monitoring (SHM), which has occupied many scientific communities over the last two decades. As a new exploring attempt to the SHM problem, this paper proposes an ant colony optimization (ACO) based algorithm for continuous optimization problems on structural damage detection in the SHM field. First of all, the theoretical background of ACO is introduced for search of approximation best solution to discrete optimization problems and further to continuous optimization problems. Then four benchmark functions are used to evaluate the performance of continuous ACO (CnACO) algorithm. After that, the problem on the structural damage detection is mathematically converted into a constrained optimization problem, which is then hopefully solved by the CnACO algorithm. Meanwhile, effect of measurement noise on the algorithm is considered in all the damage scenarios. Upon extensive numerical simulations for single and multiple damages of a 2-storey rigid frame structure, the proposed method is extended to four damage patterns of a building model of 3-storey steel frame structure made in laboratory for further experimental verification of the proposed method. Illustrated results show that the proposed method is very effective for the structural damage detection. Regardless of weak damage or multiple damages, the identification accuracy is very high and the noise immunity is better, which shows that the proposed method is feasible and effective in the SHM field.

1. Introduction

The process of implementing a damage identification strategy for engineering structures is referred to as structural health monitoring (SHM) [1]. The SHM problems have occupied many scientific communities for the last two decades [2,3]. It is to be able to detect, locate and assess the extent of damage in a structure so that its remaining life can be known and possibly extended. As an alternative to the current local inspection methods, global methods have been widely developed over the years [4]. Among the global methods, vibration-based damage detection (VBDD) techniques have been receiving increasing attention in recent years [4–6]. The basic principle of VBDD can be explained as follows. Any structure can be considered as a dynamic system with stiffness, mass and damping. Once some damage semerge in the structures, the structural parameters will change, and the frequency response functions and modal parameters of the structural system will also change. This change of modal parameters can be taken as the signal of early damage occurrence in the structural system.

Numerous damage indices, derived from damage induced changes to modal parameters, have been proposed. Briefly, they include those that rely on shifts in natural frequencies [7,8], changes in mode shapes [9], mode shape curvatures [10], measurement derived flexibility or stiffness matrices [11], modal strain energy [12], updates to numerical models to match the measured response of the damaged structure [13], and neural network based methods [14]. These studies have shown that the techniques can be used to detect the presence, location, and occasionally severity of damage on structures. However, there are still some difficulties when they are applied to the real structures, especially for that changes in the structure not due to damage, for example due to environmental effects, will be difficult to distinguish from changes due to damage [15], a significant amount of work is still required before the techniques can be routinely applied as a structural health monitoring tool for structures [3,4,6].

In essence, the most effective strategy should treat the SHM as a constrained optimization problem [16]. However, there is no universal agreement as to the optimum method for using measured vibration data for damage detection, location or quantification [3]. One of difficulties is that the traditional gradient-based methods are easily led to local rather than global minimum. Therefore, scientists are trying to explore some new approaches for the SHM problem.

* Corresponding author at: MOE Key Lab of Disaster Forecast and Control in Engineering, Jinan University, Guangzhou 510632, China. Tel.: +86 20 85220476x2012; fax: +86 20 85227932.
E-mail address: lyu1997@163.com (L. Yu).

0026-2714/$ - see front matter © 2010 Elsevier Ltd. All rights reserved.
doi:10.1016/j.microrel.2010.09.011

Please cite this article in press as: Yu L, Xu P. Structural health monitoring based on continuous ACO method. Microelectron Reliab (2010), doi:10.1016/j.microrel.2010.09.011

The use of extended continuous version of optimization technique, named ant colony optimization (ACO), is employed for the SHM problem in this paper. ACO was first introduced by Marco Dorigo in his doctoral thesis in 1992 [17] as a probabilistic technique for solving computational problems, which can be reduced to find good paths through graphs. This population-based technique is inspired in the behavior of real ants and their communication scheme by using pheromone trail. ACO has been widely used by the research community mainly due to its efficiency in solving the optimization problems, such as the traveling salesman problem [18], the routing problem in a computer network [19]. Nevertheless, the expansion to continuous variables is recent [20] and it can be seen as a new development in the history of ACO [21].

This paper is organized as follows. In Section 2, the background of ACO is presented for search of approximation solutions to discrete optimization problems and further to continuous optimization problems. In Section 3, four benchmark functions are used to evaluate the performance of continuous ACO (CnACO) algorithm. In Section 4, the proposed algorithm is applied to the optimization problem on structural damage detection, a 2-storey rigid frame is adopted to do extensive numerical simulations for single and multiple damages of the structure. In Section 5, an experimental verification of the method is implemented. Finally, a few conclusions are made, some merits on the method are also discussed.

2. Theoretical background

2.1. Ant colony optimization (ACO)

First ACO algorithms was proposed by Marco Dorigo and his colleagues in the 1990s [17–19]. More specifically, ACO is inspired by the ants' foraging behavior. At the core of this behavior is the indirect communication between the ants by means of chemical pheromone trails, which enables ants to find short paths between their nest and food sources. The characteristic of real ant colonies is exploited in ACO algorithms in order to solve, for example, discrete optimization problems or the continuous optimization problems. In general, the ACO approach attempts to solve an optimization problem by iterating the following two steps: (i) Candidate solutions are constructed in a probabilistic way by using a probability distribution over the search space. (ii) The candidate solutions are used to modify the probability distribution in a way that is deemed to bias future sampling toward high quality solutions.

The core of ACO algorithms is the pheromone model, which is a set of so-called pheromone trail parameters reflecting the search experience of the algorithm. These parameters are used to bias the solution construction over time to the regions of search space containing high quality solutions.

The choice of a solution component from the set $N(s^p)$ is done probabilistically at each construction step. The exact rules for probabilistic choice of solution components vary across different variants of ACO. The basic and the best known is that of Ant System (AS) [17]:

$$p(c_{ij}|s^p) = \frac{\tau_{ij}^{\alpha} \cdot \eta(c_{ij})^{\beta}}{\sum_{c_{il} \in N(s^p)} \tau_{il}^{\alpha} \cdot \eta(c_{il})^{\beta}}, \quad \forall c_{ij} \in N(s^p) \tag{1}$$

where τ_{ij} is the pheromone value associated with component c_{ij} and $\eta(\cdot)$ is a weighting function that assigns at each construction step a heuristic value to each feasible solution component $c_{ij} \in N(s^p)$. Furthermore, α and β are positive parameters, whose values determine the relation between pheromone information and heuristic information.

Pheromone updating is a key step of ACO. Its aim is to increase the pheromone values associated with good or promising solutions, and decrease those that are associated with bad ones. Usually, this is achieved by increasing the pheromone levels associated with chosen good solution s_{ch} by a certain value $\Delta\tau$, and by decreasing all the pheromone values through pheromone evaporation:

$$\tau_{ij} \leftarrow \begin{cases} (1-\rho)\tau_{ij} + \rho\Delta\tau & \text{if} \quad \tau_{ij} \in s_{ch}, \\ (1-\rho)\tau_{ij} & \text{otherwise} \end{cases} \tag{2}$$

where $\rho \in (0, 1]$ is the evaporation rate. Pheromone evaporation is needed to avoid too rapid convergence of the algorithm. It implements a useful form of forgetting, favoring the exploration of new areas in the search space. In principle, algorithms update pheromone using either the iteration-best solution, i.e., the best solution found in the last iteration, or the best-so-far solution, i.e., the best solution found from the start of the algorithm run (sometimes a combination of several solutions found by the ants is used). The best-so-far solution update leads to a faster convergence, while the iteration-best update allows for more diversification of the search [18,19].

2.2. ACO for continuous optimization – CnACO

When ACO is applied to combinatorial optimization problems, the set of available solution components is defined by the problem formulation. At each construction step, ants make a probabilistic choice of the solution component c_i from the set $N(s^p)$ of available components according to Eq. (1). For a continuous optimization problem, the fundamental idea underlying ACO is the shift from using a discrete probability distribution to using a continuous one, that is, a probability density function (PDF) $P(x)$, instead of choosing a component $c_{ij} \in N(s^p)$ according to Eq. (1), an ant samples a $P(x)$. The general approach to sampling $P(x)$ is to use the inverse of its cumulative distribution function $D(x)$, i.e., $D^{-1}(x)$. However, it is important to note that for an arbitrarily chosen $P(x)$, it is not always straightforward to find $D^{-1}(x)$. One of the most popular functions used as a $P(x)$ is the Gaussian function. By defining a Gaussian kernel $G^i(x)$ as a weighted sum of several one-dimensional Gaussian functions $g_l^i(x)$ as below:

$$G^i(x) = \sum_{l=1}^{k} \omega_l g_l^i(x) = \sum_{l=1}^{k} \omega_l \frac{1}{\sigma_l^i \sqrt{2\pi}} e^{-\frac{(x-\mu_l^i)^2}{2(\sigma_l^i)^2}} \tag{3}$$

where $i = 1, 2, \ldots, n$ is the number of dimensions of the problem, which identifies a single such PDF. The G^i is parameterized with three vectors of parameters: ω is the vector of weights associated with the individual Gaussian functions, μ^i the vector of means, and σ^i the vector of standard deviations respectively.

In order to obtain $G^i(x)$, three vectors ω, μ^i, σ^i are defined as follows [20],

$$\mu^i = \{\mu_1^i, \mu_2^i, \cdots \mu_{\boldsymbol{k}}^i\} = \{s_1^i, s_2^i, \cdots s_{\boldsymbol{k}}^i\} \tag{4}$$

$$\omega_l = \frac{1}{\boldsymbol{q}\boldsymbol{k}\sqrt{2\pi}} e^{-\frac{(l-1)^2}{2\boldsymbol{q}^2\boldsymbol{k}^2}} \tag{5}$$

where l is the rank of solution s_l, $\boldsymbol{k}$ is the calculation parameter, and $\boldsymbol{q}$ is a parameter of the algorithm respectively. When $\boldsymbol{q}$ is small, the best-ranked solutions are strongly preferred, otherwise the probability becomes more uniform.

$$\sigma_l^i = \xi \sum_{e=1}^{\boldsymbol{k}} \frac{|s_e^i - s_l^i|}{\boldsymbol{k} - 1} \tag{6}$$

where the algorithm parameter $\xi > 0$. The higher the value of ξ, the lower the convergence speed of the algorithm.

As mentioned before, this whole process is repeated for each dimension $i = 1, 2, \ldots, n$, and each time the average distance σ_l^i is calculated only with the use of the single dimension i. This ensures

Please cite this article in press as: Yu L, Xu P. Structural health monitoring based on continuous ACO method. Microelectron Reliab (2010), doi:10.1016/j.microrel.2010.09.011

Table 1
Benchmark functions.

Function	Function expression	Argument range	Global minimum
Sphere	$f_1(x)=\sum_{i=1}^{30}x_i^2$	$[-100, 100]$	0
Griewank	$f_2(x)=\frac{1}{400}\sum_{i=1}^{30}x_i^2-\prod_{i=1}^{30}\cos\left(\frac{x_i}{\sqrt{i}}\right)+1$	$[-600, 600]$	0
Weiestrass	$f_3(x)=\sum_{n=0}^{10}0.5^n\cos(3^n(x+0.5))$	$[-1, 1]$	0
Ackley	$f_4(x)=-20\boldsymbol{e}^{\left(-0.2\sqrt{(0.5(x^2+y^2))}\right)}+20-\boldsymbol{e}^{(0.5(\cos(2\pi x)+\cos(2\pi y))+)}-\boldsymbol{e}$	$[-5, 5]$	0

Table 2
Comparison on results based on ACO.

Function	k	m	q	ξ	n	Results
Sphere	31	12	e−04	0.85	30	9.929e−02
Griewank	35	12	e−04	0.85	30	7.924e−05
Weiestrass	21	30	e−04	0.85	10	3.309e−01
Ackley	12	8	e−04	0.85	10	1.304e−04

that the algorithm is able to adapt to linear transformations of the considered problem.

3. Benchmark function study

In order to evaluate the performance of CnACO, a suite of four famous benchmark functions are employed as shown in Table 1. Their global minimum values are all equal to zero. The CnACO is adopted to calculate the global minimum values. The algorithm coefficients used here and the calculated results are listed in Table 2. Here, $\boldsymbol{m}$ is the ant numbers, other parameters have the same meanings as ones defined in the previous section. The searching progress of the minimum values is illustrated in Fig. 1. Here, the left is the global characteristics of benchmark functions, the right the local ones. From the left ones, it seems that only the Weierstrass function is not a single-peak function. In fact, it is easy found from the right ones that only Sphere function is single-peak function and others are multi-peak function, which has multiple local minimum values.

It can be found from Table 2 and Fig. 1 that the CnACO has a good convergent properties, i.e., it can make the solution convergent to the global minimum value of the function. Therefore, the CnACO can be hopefully applied to the continuous optimization of structural damage detection in the SHM field in the following section.

4. CnACO applied to structural damage detection

The motion equation of a system with n degrees of freedom (DOFs) can be expressed as follows:

$$\boldsymbol{K}\boldsymbol{\varphi}_j=\lambda_j\boldsymbol{M}_0\boldsymbol{\varphi}_j \tag{7}$$

$$\boldsymbol{K}=\boldsymbol{K}(\boldsymbol{\alpha})=\sum_{i=1}^{N_e}\alpha_i\boldsymbol{K}_i \tag{8}$$

where $\boldsymbol{K}$ is the global stiffness matrix of a damaged structure. Since the change of mass matrix before and after damage is very small and always assumed to be unchanged in most cases, the global mass matrix of health structure $\boldsymbol{M}_0$ is used here instead of its corresponding damaged one $\boldsymbol{M}$. λ_j and $\boldsymbol{\varphi}_j$ are the j-th eigenvalue and eigenvector respectively, $j=1, 2, ..., N_m$ and N_m is the number of measured mode shapes. $\lambda_j=(2\pi f_j)^2$, and f_j is the j-th natural frequency. $\boldsymbol{K}_i$ is the i-th element stiffness matrix, and $\boldsymbol{\alpha}=[\alpha_1,\alpha_2,\ldots,\alpha_{N_e}]^T$ is the elemental stiffness parameter (ESP), which is specified to the elemental bending stiffness (EI) in this paper. N_e is the element number of the finite element model of a structure.

4.1. Objective function

In order to identify damages of structures, an objective function is defined as minimizing discrepancies between the modal results of healthy and damaged structures. The minimization of the objective function is expressed as a bound-constrained nonlinear least-squares (BCNLS) problem

$$\min_{\boldsymbol{\alpha}\in R^{N_e}}f(\boldsymbol{\alpha})=\frac{1}{2}\|\boldsymbol{r}(\boldsymbol{\alpha})\|^2=\frac{1}{2}\sum_{i=1}^{N}\boldsymbol{r}_i^2(\boldsymbol{\alpha}) \tag{9}$$

$$\boldsymbol{l}\le\boldsymbol{\alpha}\le\boldsymbol{u},\boldsymbol{r}:R^{N_e}\to R^N$$

$$\boldsymbol{r}(\boldsymbol{\alpha})_{N\times1}=\left[\boldsymbol{r}_f(\boldsymbol{\alpha})_{N_m\times1}^T,\boldsymbol{r}_\varphi(\boldsymbol{\alpha})_{N_m\times1}^T\right]^T \tag{10}$$

where $\boldsymbol{r}(\boldsymbol{\alpha})=(r_1(\boldsymbol{\alpha}), r_2(\boldsymbol{\alpha}), \ldots, r_N(\boldsymbol{\alpha}))^T$, is a N-dimensional vector-valued function, $N=2N_m\geqslant N_e$. $\boldsymbol{l}$, $\boldsymbol{u}$ are vectors of lower and upper bound, respectively. In this paper, all components of $\boldsymbol{l}$ and $\boldsymbol{u}$ are set to be 0 and 1 respectively for the purpose of damage detection. $\boldsymbol{r}_f(\boldsymbol{\alpha})$ is a N_m-dimensional vector denoting the difference of frequency ratio before and after damage. $\boldsymbol{r}_\varphi(\boldsymbol{\alpha})$ is a vector containing the modal assurance criterion (MAC) [16] of each tested mode shape with N_m dimension, where mode shapes with only measured DOFs are used and mode shape expansion is not required here. The formulas of $\boldsymbol{r}_f(\boldsymbol{\alpha})$ and $\boldsymbol{r}_\phi(\boldsymbol{\alpha})$ are given as, respectively,

$$\boldsymbol{r}_f^i(\boldsymbol{\alpha})=\left|1-\frac{f_a^i(\boldsymbol{\alpha})}{f_t^i}\right|,\quad \boldsymbol{r}_\varphi^i(\boldsymbol{\alpha})=\frac{(\boldsymbol{\varphi}_t^{iT}\boldsymbol{\varphi}_a^i(\boldsymbol{\alpha}))^2}{(\boldsymbol{\varphi}_t^{iT}\boldsymbol{\varphi}_t^i)(\boldsymbol{\varphi}_a^i(\boldsymbol{\alpha})^T\boldsymbol{\varphi}_a^i(\boldsymbol{\alpha}))} \tag{11}$$

Here f^i and $\boldsymbol{\varphi}^i$ are the i-th natural frequency and mode shape, $i=1, 2, \ldots, N_m$, subscripts t and a denote tested and analytical data respectively.

4.2. Numerical simulations

A 2-storey rigid frame structure is used to study structural damage detection based on the CnACO algorithm, some numerical simulations are conducted in this paper. Fig. 2 shows the finite element model of the frame with its corresponding dimensions. The numbers in the box indicate the element number and the others near to the frame indicate the node number. The frame was modeled by eighteen 2-dimensional beam elements with equal length. The properties of materials are as follows: elastic modulus for vertical column and horizontal beam, $E_c=E_b=2.0\times10^{11}$ N/m^2, cross-section inertial moments $I_c=0.0000126$ m^4, $I_b=0.0000236$ m^4, cross-section areas, $A_c=0.00298$ m^2, $A_b=0.0032$ m^2, material densities, $d_c=8590$ kg/m^3, $d_b=7593$ kg/m^3, where the subscripts c and b represent column and beam respectively.

In order to simulate the structural damage cases, a single and multi-damage of the frame are specified. First five natural frequencies and mode shapes are taken into consideration for the damage detection calculation.

For the CnACO algorithm used here, the iteration number is set to be 10,000 for both the single damage cases and the multi-damage cases. Further, in order to simulate more realistic

Please cite this article in press as: Yu L, Xu P. Structural health monitoring based on continuous ACO method. Microelectron Reliab (2010), doi:10.1016/j.microrel.2010.09.011

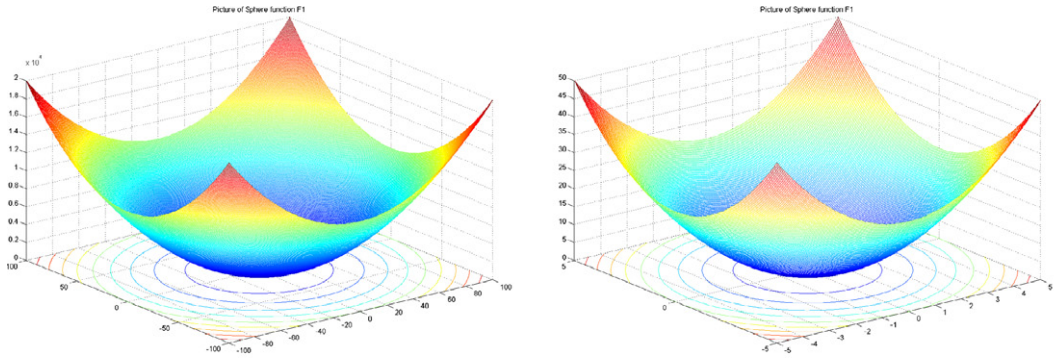

(a) Sphere function

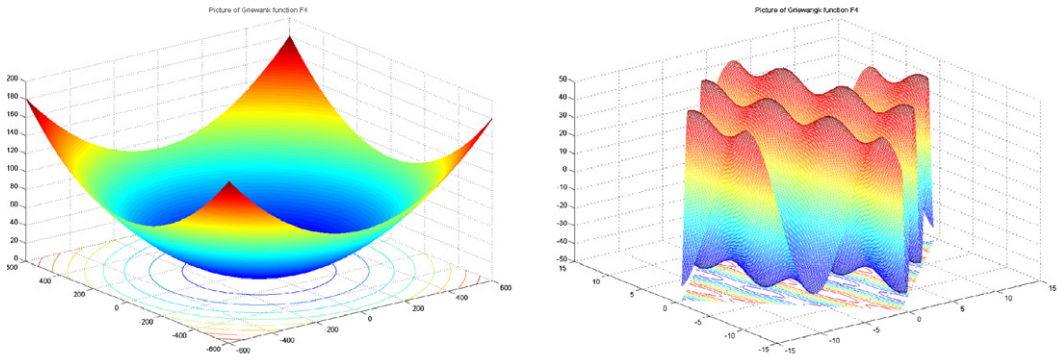

(b) Griewank function

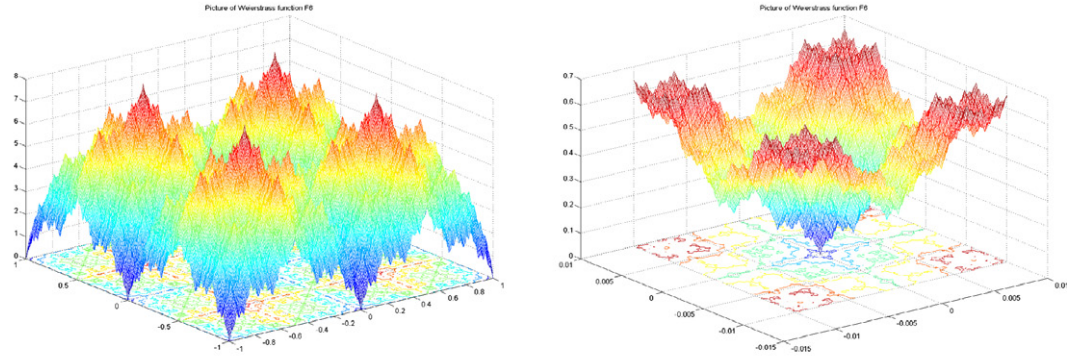

(c) Weierstrass

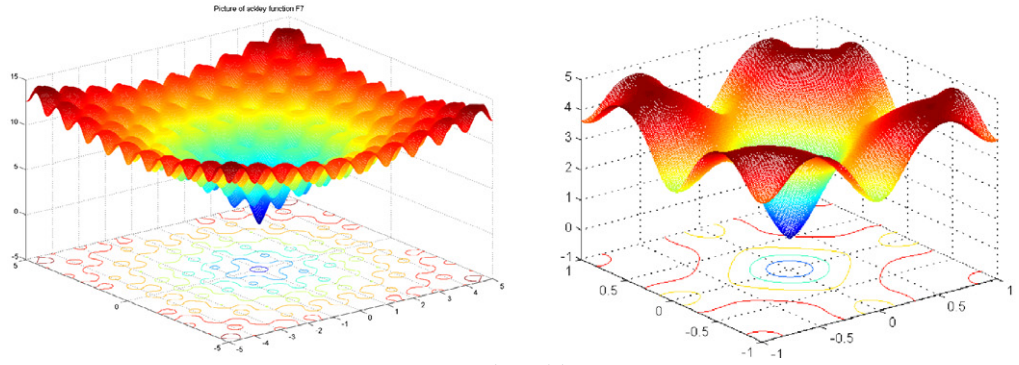

(d) Ackley

Fig. 1. Benchmark function minimum. Note: left ones is for global characteristics, right ones for local ones.

cases with contaminated measurement noise, the mode shapes are corrupted with a normally distributed random noise with different levels of 5% and 10% respectively in the same way as ones in the Ref. [22] for both the single and multi-damage cases.

Please cite this article in press as: Yu L, Xu P. Structural health monitoring based on continuous ACO method. Microelectron Reliab (2010), doi:10.1016/j.microrel.2010.09.011

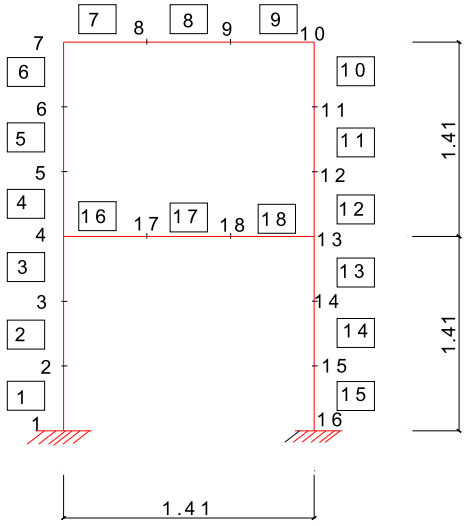

Fig. 2. Finite element model of frame (dimension in m).

4.2.1. Single damage detection

There are two scenarios in this case. One considers normal damage with an extent of 3%, 5%, 10% and 15% at a specified element respectively. The other considers weak damage with an extent of 0.5% and 1% respectively. The 8th and 17th elements are set to be the damage ones. Table 3 shows the scenarios and the damage detection results. Where, capital letter NL indicates Noise Level contaminated in the mode shapes, for example. NL = 5, means 5% noise is contaminated into the mode shapes. Damage extent symbol 3@17 indicates 3% reduction of stiffness at element 17. Same recognition can be found in the following tables. It is found from Table 3 that the lowest accuracy occurs in the case of 0.5@17, i.e., 0.5% stiffness reduction at 17th element. Its corresponding damage detection result is shown in Fig. 3, in which the first white bar from left is for the case of true damage, the others are for the damaged cases with different noise levels. Same legend is used for the figures in the following sections.

It can be seen from Table 3 and Fig. 3 that: (a) the proposed ACO-based algorithm is a precise method. The structural damage detection under all the cases is precise, the higher the damage extent is, the better the damage detection results are; (b) even for the case of weak damage of 0.5% at 17th element, the lowest accuracy case, the accuracy is higher than 80%, which shows that the proposed algorithm can not only locate the damage but also quantify the damage extent; (c) the effect of noise on the algorithm is not so significant, or says the algorithm has a good immunity to the noise, but the convergent rate is associated with the noise level.

Table 3
Single damage detection results.

True damage (%)		Damage detection (%)	Accuracy
Extent	NL		
3@17[a]	0	2.96@17	98.7%
	5	2.96@17	98.7%
	10	2.97@17	99.0%
5@17	0	4.99@17	99.8%
	5	4.99@17	99.8%
	10	4.99@17	99.8%
10@17	0	10@17	100%
	5	10@17	100%
	10	10@17	100%
5@8	0	4.99@8	99.8%
	5	5.00@8	100%
	10	4.99@8	99.8%
10@8	0	10@8	100%
	5	10@8	100%
	10	10@8	100%
0.5@17	0	0.42@17	84%
	5	0.42@17	84%
	10	0.40@17	80%
1.0@17	0	0.92@17	92%
	5	0.96@17	96%
	10	0.97@17	97%
0.5@8	0	0.42@8	84@
	5	0.44@8	88%
	10	0.46@8	92%
1.0@8	0	0.97@8	97@
	5	0.96@8	96@
	10	0.95@8	95%

[a] *Notes*: 3@17 indicates 3% reduction of stiffness at 17th element.

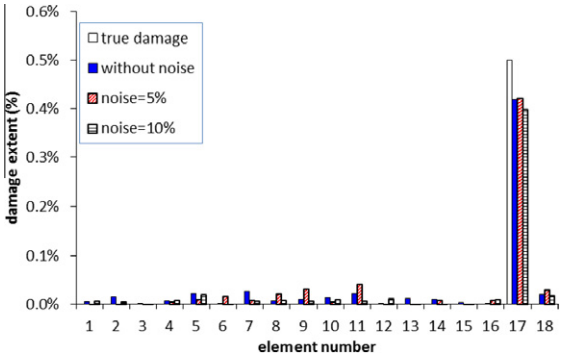

Fig. 3. Single damage detection under the lowest accuracy case.

4.2.2. Multi-damage detection

4.2.2.1. Two-damage detection. For two-element damage scenarios, stiffnesses at both the 8th and 17th elements are set to be reduced by different damage extents simultaneously. Six cases are listed here, they are (10%, 10%), (10%, 20%), (10%, 25%), (20%, 20%), (25%, 10%) and (20%, 10%) respectively. For example, case (10%, 25%) means stiffness at 8th element is set to be reduced by 10% while the 17th element reduced by 25% simultaneously. The damage detection results are listed in Table 4. It can be found from Table 4 that the proposed method can correctly identify the two damages, but there are also wrong indicators at the undamaged elements at the same time. For the worst identification case, i.e., (20%, 20%), damaged at 8th and 17th elements by 20% simultaneously, the damage detection results are shown in Fig. 4, which indicates that two damaged 8th and 17th elements can be correctly found with a better accuracy but there also appear two wrong spikes at two undamaged 5th and 11th elements, particularly for the case of noise level NL = 10%.

From Table 4 and Fig. 4, it can be seen that: (a) the proposed ACO-based algorithm is a very effective method for the identification of two damages, it can not only effectively locate but also quantify the two damages for all the cases; (b) if damage extents at 8th and 17th elements are different, the detection results are better than ones for the same damage extents occur at two elements simultaneously; (c) the algorithm can give few wrong indicator at 5th and/or 11th elements, especially for the cases with same damage extents at 8th and 17th elements; (d) noise level affects the detection results, the damage identification accuracy decrease as the noise level increase, and the convergent rate is associated with the noise level.

Please cite this article in press as: Yu L, Xu P. Structural health monitoring based on continuous ACO method. Microelectron Reliab (2010), doi:10.1016/j.microrel.2010.09.011

4.2.2.2. Multi-damage detection. Some cases for more than two damaged elements are also considered in this section so that the performance of the proposed ACO-based algorithm applied to the cases can be evaluated. For example, three-element damage detection results are shown in Fig. 5 and four-element damage detection

Table 4
Two-damage detection results.

True damage (%)		Damage detection (10%)	
Extent	NL	Correct location	Wrong location
10@8[a]	0	9.2@8, 9.0@17	0.8@5, 1.2@11
10@17	5	8.4@8, 8.2@17	1.4@5, 2.4@11
	10	7.8@8, 7.2@17	4.2@5, 2.1@11
10@8	0	7.5@8, 18@17	4@5, 3.5@11
20@17	5	9@8, 19.5@17	2@11
	10	6.5@8, 17@17	3.5@5, 7@11
10@8	0	10@8, 25@17	
25@17	5	6.5@8, 22@17	5@5, 4@11
	10	7.5@8, 23.5@17	6@5
20@8	0	18.8@8, 18.5@17	2@5, 3@11
20@17	5	17.5@8, 17.2@17	3@5, 5@11
	10	16.5@8, 16@17	1.5@5, 9@11
25@8	0	24.5@8, 9.5@17	1@5
10@17	5	23@8, 6.52@17	5.5@5, 2@11
	10	22.6@8, 6.3@17	3.5@5, 5@11
20@8	0	18@8, 8@17	3@5, 1.5@11
10@17	5	19.5@8, 9.5@17	1.5@5
	10	20@8, 10@17	

[a] *Notes*: 10@8 indicates 10% reduction of stiffness at 8th element.

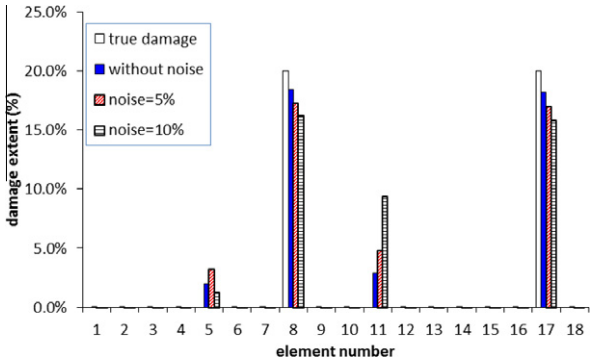

Fig. 4. Detection results for 8th and 17th elements damaged by 20% simultaneously under the worst identification case.

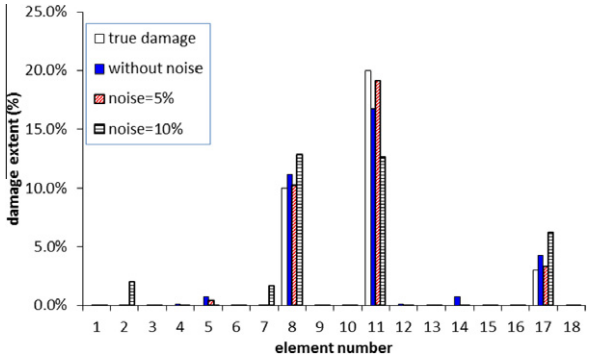

Fig. 5. Detection results for 8th element damaged by 10%, 11th by 20%, and 17th by 3% simultaneously.

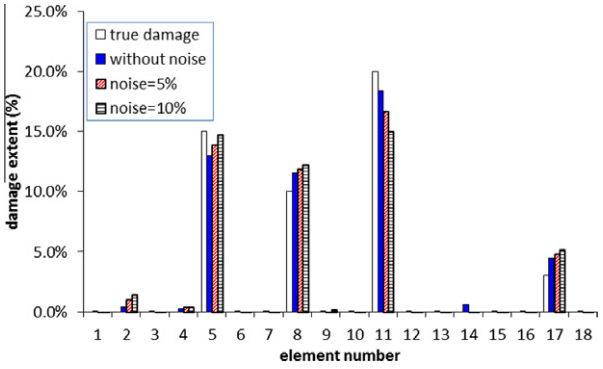

Fig. 6. Detection results for 5th element damaged by 15%, 8th by 10%, 11th by 20%, and 17th by 3% simultaneously.

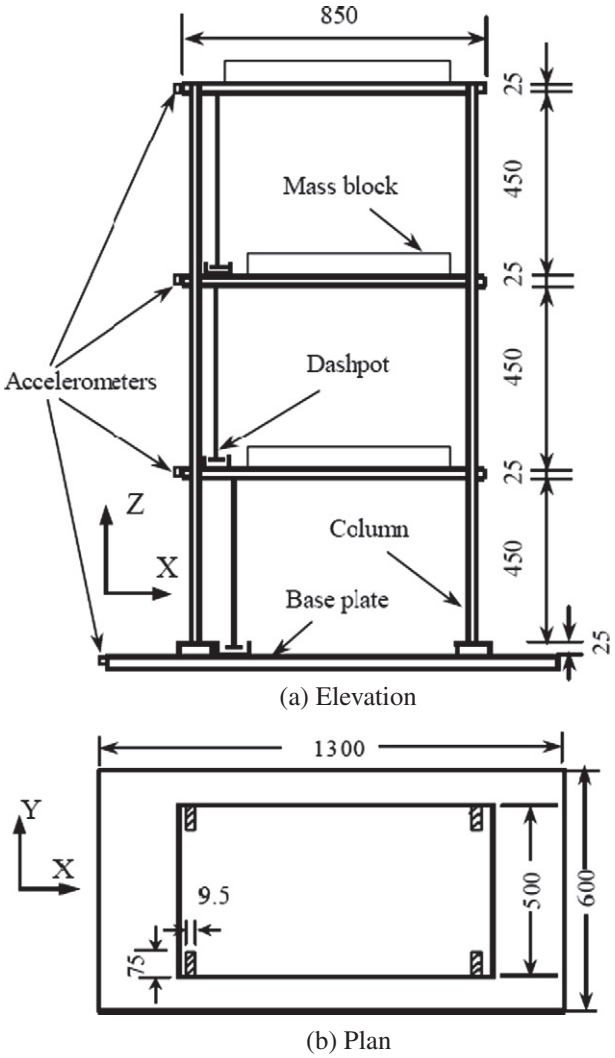

Fig. 7. Configuration of 3-storey frame model (all dimensions in mm).

Table 5
Natural frequencies (Hz) of health structure.

Modal No.	Experimental	Initial analytical	Updated analytical
1	3.369	3.554 (5.491%)	3.378 (0.267%)
2	9.704	9.957 (2.607%)	9.664 (0.412%)
3	14.282	14.389 (0.749%)	14.253 (0.203%)

Notes: The values in parentheses denote error (%) between analytical and experimental natural frequencies.

Please cite this article in press as: Yu L, Xu P. Structural health monitoring based on continuous ACO method. Microelectron Reliab (2010), doi:10.1016/j.microrel.2010.09.011

Table 6
Damage patterns of 3-storey frame model.

Storey No.	Undamaged		Damage patterns							
			(i)		(ii)		(iii)		(iv)	
	b/mm	SRE	b/mm	SRE	b/mm	SRE	b/mm	SRE	b/mm	SRE
1	75	0	51.30	11.6%	37.46	21.1%	37.46	21.1%	37.46	21.1%
2	75	0	75	0	75	0	51.30	11.6%	37.46	21.1%
3	75	0	75	0	75	0	75	0	75	0

Notes: SRE denotes stiffness reduction extent, which is computed based on shear-building assumptions.

results in Fig. 6. The illustrated results show that the proposed algorithm is very effective method for multi-damage cases as well. It can not only effectively locate but also quantify multi-element damages simultaneously.

5. Experimental verification

In order to further evaluate the proposed method in laboratory condition, a simple 3-storey building steel frame [23] is adopted. The effectiveness of the proposed method on the laboratory building model is investigated here.

5.1. Configuration of 3-storey steel frame

The 3-storey building frame was fabricated using three steel plates of $850 \times 500 \times 25$ mm^3 with four equally sized rectangular columns of 9.5×75 mm^2 as shown in Fig. 7. The plates and columns were properly welded to form rigid connections. The building model was then welded on a steel base plate of 20 mm thickness. The steel base plate was in turn bolted firmly on a shaking table using a total of eight bolts of high tensile strength. The overall dimensions of the building were $1450 \times 850 \times 500$ mm^3. All the columns were made of high strength steel of 435 Mpa yield stress and 200 Gpa modulus of elasticity. The 9.5×75 mm^2 cross-section of the column was arranged in such a way that the first natural frequency of the building was much lower in the x-direction than in the y-direction. This arrangement restricted the building motion in the x-direction and thus the building was effectively reduced to planar building in the x–z plane. The thickness of each steel floor was 25 mm so that the floor can be regarded as a rigid plated in the horizontal direction, leading to a shearing type of deformation. The geometric scale of the building model was assumed to be 1/5. To do a better simulation, an additional mass block of 135 kg was placed on each floor of the building model.

The building model was subjected to a white noise random ground excitation generated by a 3×3 m^2 MTS shaking table of the Hong Kong Polytechnic University. Each building floor was equipped with one B&K 4370 accelerometer in the x-direction. The signals from the accelerometers was analyzed by commercial computer software ARTeMIS, developed by Structural Vibration Solutions in Denmark, to identify the modal parameters (natural frequencies and mode shapes) using the method of Frequency Domain Decomposition (FDD). Since this frame can be simplified as a 3-DOF shear-building model, all the three modes can be measured ($N_m = 3$), and thus utilized in the following identification process.

5.2. Finite element model and its updating

Table 5 compares the analytical natural frequencies with the experimental results. From this table, it can be seen that the differences between the initial analytical frequencies and the experimental results from the healthy structure are obvious, and the maximum error is 5.491%, which occurs at the first mode. Thus the model updating process is performed before the damage detection procedure is carried out. The elemental stiffness parameter (ESP), i.e., the elemental Young's modulus, of each storey is considered as the updating parameter, and the number of unknown model parameters is 3. Since the dimension of objective function vector ($2N_m$) is larger than the number of unknown parameters (i.e., $6 > 3$), no expansion of objective function is required for this model. After the model updating, the natural frequencies calculated from the updated FE model are very close to the corresponding measured results as shown in Table 5. The updated FE model is then adopted in the following damage detection procedure.

5.3. Damage detection

Four damage patterns considered in the experimental studies are shown in Table 6. They were implemented step by step by cutting the width of the columns, i.e., b as shown in Fig. 8, in the first storey to 51.30 mm (pattern i) and then to 37.46 mm (pattern ii) within a height of 60 mm from the bottom, followed by cutting the width of the columns in the second storey to 51.30 mm (pattern iii) and then to 37.46 mm (pattern iv) within a height of 60 mm from the second floor. The measured natural frequencies before and after damage for each damage pattern are listed in Table 7.

Since the identification model of the 3-storey frame structure (i.e., a 3-storey shear-building model) is simple, the computational effort is very small by using the proposed ACO-based damage detection method, and the convergence can be quickly achieved for all damage patterns. The damage identification results for all damage patterns are shown in Fig. 9. It is very clear that both the identified damage location and extent are very close to the true ones, which shows that the proposed method is a very effective.

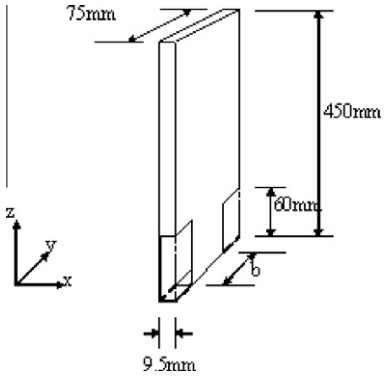

Fig. 8. Details of damaged column.

Please cite this article in press as: Yu L, Xu P. Structural health monitoring based on continuous ACO method. Microelectron Reliab (2010), doi:10.1016/j.microrel.2010.09.011

Table 7
Measured natural frequencies (Hz) before and after damage.

Modal No.	Undamaged	Damage patterns			
		(i)	(ii)	(iii)	(iv)
1	3.369	3.259 (3.265%)	3.113 (7.599%)	3.076 (8.697%)	3.003 (10.864%)
2	9.704	9.485 (2.257%)	9.302 (4.143%)	9.192 (5.276%)	9.082 (6.410%)
3	14.282	14.209 (0.511%)	14.136 (1.022%)	13.660 (4.355%)	13.330 (6.666%)

Notes: Values in parentheses denote error (%) between measured natural frequencies from undamaged and damaged frames.

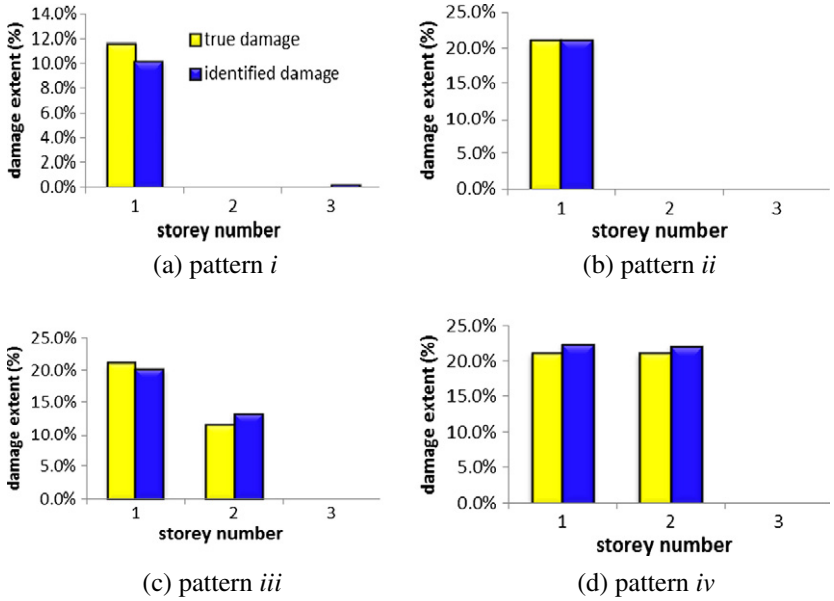

Fig. 9. Comparison on results of true and identified damage.

6. Conclusions

Some issues on structural health monitoring (SHM) are studied based on continuous ant colony optimization (CnACO) method in this paper. The basic ACO is first introduced for search of approximation best solution to discrete optimization problems and further to continuous optimization problems. Then four benchmark functions are used to evaluate the performance of CnACO algorithm. After that, an objective function for structural damage detection is defined as minimizing the discrepancies between the modal data of healthy and damaged structures, the problem on the structural damage detection is converted into a constrained optimization problem in mathematics, and further solved by the CnACO algorithm. A 2-storey rigid frame is adopted to do extensive numerical simulations for single and multiple damages of the structure. Experimental verification of four damage patterns of a 3-storey building model in laboratory is also conducted for further evaluation of effectiveness and robustness of the proposed method. The illustrated results show that the ACO-based method is very effective for the SHM problem. Regardless of weak damage or multiple damages, the proposed algorithm has an good identification accuracy and a good immunity to the measurement noise. It can not only locate the structural damages but also quantify the severity of damages, which shows that the ACO-based algorithm is feasible and effective in the SHM field. However, when the algorithm updates the pheromone, there are significant influence between using the iteration-best solution and by the best-so-far solution, especially for the large scale problem. Therefore, the hybridization of ACO algorithms with more classical artificial intelligence and operations research methods are required in the future.

Acknowledgments

The project is jointly supported by the National Natural Science Foundation of China (Grant Nos. 50978123 and 11032005), the Guangdong Natural Science Foundation (Grant No. 10151063201000022) and the Fundamental Research Funds for the Central Universities (Grant No. 21609601).

References

[1] Farrar CR, Worden K. An introduction to structural health monitoring. Philos Trans Royal Soc A 2007;365:303–15.
[2] Sohn H, Farrar CR, Hemez FM. A review of structural health monitoring literature: 1996–2001. LA-13976-MS, New Mexico: Los Alamos National Laboratory Report; 2003.
[3] Gul M, Catbas FN. Statistical pattern recognition for Structural Health Monitoring using time series modeling: Theory and experimental verifications. Mech Syst Signal Process 2009;23:2192–204.
[4] Alvandi A, Cremona C. Assessment of vibration-based damage identification techniques. J Sound Vib 2006;292:179–202.
[5] Yan Y, Cheng L, Wu Z, Yam L. Development in vibration-based structural damage detection technique. Mech Syst Signal Process 2007;21:2198–211.
[6] Carden E, Fanning P. Vibration based condition monitoring: a review. Struct Health Monit 2004;3(4):355–77.
[7] Doebling SW, Farrar CR, Prime MB, Shevitz DW. Damage identification and health monitoring of structural and mechanical systems from changes in their vibration characteristics: a literature review, technical report. Research report LA-13070-MS, Los Alamos National Laboratory; 1996.
[8] Adams RD, Cawley R. The localization of defects in structures from measurements of natural frequencies. J Strain Anal 1979;14:49–57.
[9] Fox CHJ. The location of defects in structures: a comparison of the use of natural frequency and mode shape data. In: Proc., 10th int. modal analysis conf. society of experimental mechanics, Bethel, Conn.; 1992. p. 522–8.
[10] Zhang Z, Aktan AE. Application of modal flexibility and its derivatives in structural identification. Res Nondestruct Eval 1998;10(1):43–61.

Please cite this article in press as: Yu L, Xu P. Structural health monitoring based on continuous ACO method. Microelectron Reliab (2010), doi:10.1016/j.microrel.2010.09.011

[11] Zimmerman DC, Kaouk M. Structural damage detection using a minimum rank update theory. J Vib Acoust 1994:222–31.
[12] Kim JT, Stubbs N. Nondestructive crack detection algorithm for full-scale bridges. J Struct Eng 2003;129(10):1358–66.
[13] Casas JR, Aparicio AC. Structural damage identification from dynamic-test data. J Struct Eng 1994;120(8):2437–50.
[14] Wu X, Ghaboussi J, Garrett JH. Use of neural networks in detection of structural damage. Comput Struct 1992;42(4):649–59.
[15] Sohn H, Worden K, Farrar CR. Statistical damage classification under changing environmental and operational conditions. J Intell Mater Syst Struct 2002;13(9):561–74.
[16] Yu L, Wan ZY, Xu DY, Zhu HP. An improved PSO algorithm for structural damage detection. In: Proc. 1st int. conf. on structural condition assessment, monitoring and improvement (SHM05). Perth, W. Australia, December 12–14, 2005. p. 99–105.
[17] Dorigo M. Optimization, learning and natural algorithms [in Italian], PhD Thesis, Politecnico di Milano, Italy; 1992.
[18] Dorigo M, Gambardella LM. Ant colony system: a cooperative learning approach to the traveling salesman problem. IEEE Trans Evolut Comput 1997;1(1):53–66.
[19] Di Caro G, Dorigo M. Ant net: distributed strigmergic control for communication networks. J Artif Intell Res 1998;9:317–65.
[20] Socha K. ACO for continuous and mixed-variable optimization. In: Dorigo M, editors. Proc. in ANTS 2004 – fourth international workshop on ant colony optimization and swarm intelligence, Brussels, Belgium; 2004.
[21] Viana FAC, Kotinda G, Rade DA, Steffen V. Tuning dynamic vibration absorbers by using ant colony optimization. Comput Struct 2008;86:1539–49.
[22] Yu L, Yin T. Damage identification in frame structures based on model updating. J. Vib Acoust 2010;132:051007.
[23] Zhu HP, Xu YL. Damage detection of mono-coupled periodic structures based on sensitivity analysis of modal parameters. J Sound Vib 2005;285(1):365–90.

Please cite this article in press as: Yu L, Xu P. Structural health monitoring based on continuous ACO method. Microelectron Reliab (2010), doi:10.1016/j.microrel.2010.09.011